Organic matter from Arctic sea ice loss alters bacterial community structure and function

(in press) *Nature Climate Change*

Authors: Graham J. C. Underwood[1]*†, Christine Michel[2]†, Guillaume Meisterhans[2], Andrea Niemi[2], Claude Belzile[3], Matthias Witt[4], Alex J. Dumbrell[1], Boris P. Koch[5,6]

Affiliations:

[1] School of Biological Sciences, University of Essex, Colchester, Essex, U.K. CO4 3SQ.

[2] Fisheries and Oceans Canada, Freshwater Institute, 501 University Crescent, Winnipeg, Manitoba, R3T 2N6, Canada.

[3] Institut des sciences de la mer de Rimouski, Université du Québec à Rimouski, 310 Allée des Ursulines, Rimouski, Quebec, G5L 3A1, Canada.

[4] Bruker Daltonik GmbH, Fahrenheitstraße 4, 28359 Bremen, Germany.

[5] Alfred-Wegener-Institut Helmholtz-Zentrum für Polar- und Meeresforschung, Am Handelshafen 12, 27570 Bremerhaven, Germany.

[6] University of Applied Sciences, An der Karlstadt 8, 27568 Bremerhaven, Germany.

† these authors contributed equally to this work.

Abstract

Continuing losses of multi-year sea ice (MYI) across the Arctic are resulting in first-year ice (FYI) dominating the Arctic ice pack. Melting FYI provides a strong seasonal pulse of dissolved organic matter (DOM) into surface waters; however, the biological impact of this DOM input is unknown. Here we show that DOM additions cause significant and contrasting changes in under-ice bacterioplankton abundance, production and species composition. Utilization of DOM was influenced by molecular size, with 10-100 kDa and >100 kDa DOM fractions promoting rapid growth of particular taxa, while uptake of sulfur and nitrogen-rich low molecular weight organic compounds shifted bacterial community composition. These results demonstrate the ecological impacts of DOM released from melting FYI, with wide-ranging consequences for the cycling of organic matter across regions of the Arctic Ocean transitioning from multi-year to seasonal sea ice as the climate continues to warm.

The Arctic is undergoing accelerated warming (*1*), resulting in changes to the areal extent and age profile of sea ice. Thick ice that persisted over multiple years (multi-year ice, MYI) is being replaced by thinner seasonal first-year ice (FYI) (*2-4*), significantly changing the ecology and biogeochemistry of the Arctic Ocean (*5, 6*). FYI hosts productive microbial assemblages that accumulate large amounts of dissolved organic matter (DOM) (*7-10*), and support important ice-associated food webs (*11*). Increased seasonal melting of FYI ice and the predicted complete shift from MYI to FYI in the Arctic (*12*), and significant differences in richness and diversity between MYI, FYI, and underlying seawater bacterial communities (*13, 14*), suggests that under-ice microbial communities may be affected by sea ice DOM inputs, though rates of utilization and degree of selectivity by bacterial planktonic assemblages remain to be determined. Determining the cycling and role of the ice-derived DOM pool in affecting water column microbial assemblages, will improve our understanding of biogeochemical cycling in an Arctic significantly altered by climate change.

DOM influences the physical structure of sea ice (*7, 8*), with organic matter held within brine channels in various molecular size configurations (a continuum of dissolved, colloids, and gels (*10, 15, 16*)). These substances are released into the surface waters upon ice melt (*6, 17, 18*). Differential retention of dissolved and gel organic fractions in ice means that organic fluxes vary during the melt period (*18, 19*). Concentrations of dissolved organic carbon (DOC) at the time of ice melt in surface waters can be high; > 250 μmol L^{-1} in under-ice surface waters of the Canadian Archipelago and the Beaufort Sea, (*20, 21, 22*), 300 μmol L^{-1} near Barrow, Alaska (*19*). However, the fate of these DOM constituents once released into the under-ice surface water remains an open question. In the seasonally stratified under-ice water column, ice-derived DOM is utilized by bacterioplankton, contributing to its biogeochemical cycling during the early-ice melt period (*6, 23, 24*), and to carbon burial (*25*) and aerosol formation (*26*). Bacterioplankton off Svalbard derived 59% of their carbon

requirements from ice-algal carbon, despite other carbon sources being available (*27*). Sea ice DOM also has a priming effect, enhancing the degradation of riverine DOM in seawater (*28*), emphasizing the important seasonal role of DOM release from sea ice in microbial biogeochemical cycling in Arctic surface waters (*6*, *11*).

We tested the hypothesis that addition of different Arctic sea ice DOM fractions at concentrations similar to those measured under ice during ice melt would alter the diversity and structure of the under-ice bacterioplankton community, and influence carbon turnover of different organic constituents. We isolated fresh sea ice DOM from the algal-rich bottom layer of FYI. This layer contains over 90% of the algal biomass present in the entire ice profile (*29*) and high concentrations of DOM, containing a spectrum of molecular size classes including extracellular polymeric substances (EPS) produced by sea ice diatoms (*9, 10, 30, 31*). Using differential molecular weight filtering, we obtained three fractions: (i) sea-ice derived DOM filtered through GF/F filters (termed "DOM_{tot}" in the following); (ii) a high molecular weight DOM fraction (HMW) retained on a 100 kDa filter and (iii) a lower molecular weight (LMW) retained between 10 kDa and 100 kDa filters. These three fractions were added to independent replicate microcosms containing natural under-ice seawater (30 per treatment) incubated at *in situ* temperatures. We followed microbial community responses over 9 days in terms of substrate utilization, bacterial growth and changes in taxonomic composition, determined by NGS (Ion PGM and 454) sequencing of 16S rRNA genes. We applied solid-phase extraction followed by ultra-high resolution Fourier transform ion cyclotron resonance mass spectrometry (FT-ICR-MS) to characterize the changes in elemental composition and utilization of DOM of the treatments. The analytical window for this characterization covered molecular masses from 200 to 600 Da (*32*).

Results and Discussion

Under-ice seawater contained 60 µmol L^{-1} dissolved organic carbon (DOC), as previously reported for Arctic waters (*24*, *33*). DOM_{tot}, HMW and LMW additions significantly increased DOC concentrations compared to controls (Fig. 1a, Table S1), to values within the range of DOC measured under sea ice during ice melt (*19*, *24*, *21*, *22*, *20*). The treatments contained higher concentrations of DOM than in enrichment studies using MYI (*17*), due to the higher diatom-dominated algal biomass, and predominance of diatom-derived DOM and EPS in the bottom layers of FYI at this site and in the Canadian Archipelago (*10*, *29*, *34*, *35*). In the DOM_{tot} addition, DOC and dissolved carbohydrates (dCHO) had similar enrichment factors, whereas DOC enrichment was greater than that of dCHO in the HMW and LMW additions (Table S1). Up to 68% of the dCHO in bottom ice is < 8 kDa (*10*), which was not preferentially retained by the molecular filters in both HMW and LMW treatments. Low molecular weight (< 600 Da) solid-phase extractable organic compounds were present in all four treatments, and their molecular formulas were identified using FT-ICR-MS (Fig. S2). The <600 Da sea-ice DOM_{tot} fraction included a large number of unique formulas (Table S1), especially compounds with higher H:C and C:N but lower O:C and C:S ratios, compared to the background seawater DOM (Fig. S2, Table 1, Table S1. The HMW and LMW additions altered the molecular formula composition of the <600 Da fraction, with unique compounds added in both treatments). We assume that these smaller monomers can form intermolecular aggregates (*15*, *36*) that are retained by membrane-based separation techniques and therefore present in the added material. Key differences in the organic matter profiles between the DOM_{tot}, HMW and LMW treatments were a greater proportion of EPS-carbohydrate (16 - 24% of dCHO, Table S1), and higher DOC:DON (dissolved organic nitrogen) ratios (Fig. S1) in the HMW and LMW additions. This is evidence that these molecular filter cut offs retained the EPS produced by ice-diatoms (*10*, *31*), which are the

dominant autotrophs in FYI in our study region (*10*, *37*, *38*). DOM_{tot} additions showed higher concentrations of dCHO (but a lower % contribution of higher molecular weight EPS constituents), higher numbers of unique molecular formulas <600 Da, and higher DON concentrations (Fig. 1b, Table S1). The different additions therefore provided a range of DOM sources, encompassing the spectrum described by the size-reactivity continuum model (*16*), and with a variety of different chemical constituents, potentially selecting for different bacterial taxa (*39-41*).

Concentrations of DOC, DON and dCHO decreased significantly in the addition treatments over 9 days (216 hours; Fig. 1a,b, Fig. S1a), with differences in the amount of organic and inorganic components utilized, and with no significant changes in concentrations in the controls (Fig. 1c, Table 1). Proportionally more dCHO (50 - 60%) was utilized compared to the overall utilization of DOC (between 13 – 40%), including in the HMW and LMW treatments (Fig. 1c), despite the carbohydrate enrichment in these treatments being lower than the overall DOC enhancement (Table S1). This indicates that bacterial growth responses were not affected solely by DOM concentration, but also DOM composition. In the HMW and LMW additions, bacterioplankton used nitrate as well as DON (Fig. 1c, S3a). Assimilation of inorganic nitrogen sources was also observed in studies where carbohydrates or mono-sugars were preferentially used for growth (*16*, *17*). However, in the DOM_{tot} addition, there was substantial utilization of DON in preference to nitrate (Figs. 1b,c, Table 1). A similar level of utilization of DON by Arctic bacterioplankton was observed in addition experiments using riverine DOM (*42*). DOC:DON ratios increased with time, with the HMW and LMW treatments showing the greatest increases (Fig. S1b).

There were no significant differences in bacterial density at T0 between treatments and controls (Fig. 2). HMW and LMW additions stimulated logarithmic bacterial growth, with peak bacterial production occurring from 144 to 216 h (Figs. 2a,b) and intrinsic growth

rates comparable to the higher end of those reported in the Arctic (*43*). The DOM_{tot} additions had a significant lag phase, before bacterial growth reached rates ($\mu = 0.35\ day^{-1}$) comparable with the HMW and LMW treatments at 192 h. In the controls, bacterial cell densities doubled once over the 9 day experiment, with low bacterial production (Fig. 2b) and low intrinsic growth rates ($\mu < 0.05\ d^{-1}$), similar to densities and growth rates in natural Arctic bacterioplankton summer communities ($\mu = 0.038$ to $0.08\ d^{-1}$) (*43, 44*).

The degradation of organic matter is influenced by chemical composition, size and reactivity, and the ability of microorganisms to synthesize extracellular enzymes for the hydrolysis of larger compounds (*16, 45*). Within the spectrum of sea-ice DOM provided, the greatest proportional utilization was of dCHO in the HMW and LMW treatments containing a high fraction of EPS (originating from ice diatoms, *10, 31*). This large utilization occurred despite the presence of higher concentrations of other, lower molecular weight, material (Fig. 1d). Apparent substrate utilization (femtomol C or N per bacterial cell) were lower (*i.e.* more efficient) in the HMW and LMW treatments, and lower for dCHO compared to DOC in each treatment (Table 1) though within ranges for marine bacteria (*46*). Proportionally more carbohydrate was used to support bacterial growth than other DOM components (Fig 1c). Arctic bacterioplankton growth rates are positively correlated with DOC (up to saturating concentrations between 200 – 500 µmol C L^{-1}) and strongly influenced by the concentrations of labile components within the DOM pool (*43*). The growth rates measured in this study point to an abundance of labile components in the FYI-derived DOM. In comparison with the HMW and LMW treatments, DOM_{tot} enrichment elicited a delayed response as bacteria potentially adjusted to reduced salinity, and induction of mechanisms to access the wide pool of DON and sulfur-rich compounds present in the DOM_{tot} fraction. Many small organic compounds seem unavailable to bacteria, forming the unreactive pool of oceanic DOM (*15, 16, 47*). However, we found increased loss or transformation of <600 Da ice-derived

nitrogen- and sulfur- rich compounds, in particular in the DOM_{tot} treatment (Table 1). The number of identified molecular formulas <600 Da decreased by 6-11% in all treatments over the incubation period, though no significant changes in average molecular mass was observed (Table S2). Between 71 and 136 compounds were lost after 216 h in the additions compared to 18 compounds in the controls (Fig. 3). This suggests that in conditions representative of the stratified meltwater layers in marginal ice zones or under the ice, these small molecules can be utilized by bacterioplankton (*48*).

The utilization of nitrogen- and sulfur-containing compounds varied, with a comparable utilization of sulfur-containing compounds in the HMW and LMW (Table 1). The average C:N ratio of all detected formulas in the DOM_{tot} addition increased by 17%, while remaining similar in the HMW and LMW treatments. Preferential removal of sulfur-containing compounds increased C:S ratios in all treatments (Table 1, Table S1). Although the overall average O:C ratio was unchanged in the HMW and LMW treatments, formulas which showed the strongest relative peak magnitude increase in the HMW addition were highly oxidized compounds (higher O:C ratio, Fig. 3c), a trend which was not observed in LMW fraction (Fig. 3d).

The T0 bacterioplankton assemblages had a high taxonomic richness (Fig. 4a), with major constituents being Pelagibacteraceae, Rhodobacteraceae, Alteromondales, Oceanospirillales, *Polaribacter* and *Tenacibaculum* (Fig. 4c, Fig. S4); a taxonomic profile similar to that of under-ice bacterioplankton in this (*49*), and other, Arctic regions (*13, 42, 50, 51*). After 216 hours incubation, seawater controls showed minor losses of taxonomic richness, compared with major declines in taxonomic richness in the three addition treatments (Fig 4a, Kruskal-Wallis, $P < 0.01$). Dominant bacteria in controls at T216 were a single Pelagibacteraceae OTU (which increased in relative abundance from T0 to T216), Rhizobiales and Rhodospirillales (*Roseomonas*), *Oxalicibacterium* (3.5% of the T216 control

assemblages, and three *Colwellia*, a *Moritella* and an unidentified Oceanospirillales OTU (Fig. 4c). These OTUs may have been present, but unidentified at T0, due to lower levels of taxonomic resolution at T0 compared to T216 resolution (the relative abundance of higher taxonomic groupings at T0 match the relative abundance of lower taxonomic level OTUs within those groupings at T216). Low relative abundance of Rhodobacteraceae OTUs (2.4 % at T0, and 0.6% overall at T216), and a single Pelagibacteraceae OTU in our samples may reflect the coastal conditions in the Canadian Archipelago. Potential primer bias against these groups has been reported (*42*, *52*), although the primers we used do amplify these groups (*41*, *53*). In comparison, high abundances of Rhodobacteraceae and SAR11 clades were found in open ocean samples (*50*). These changes, coupled with the measured growth rates and cell densities (Fig. 2a,b), indicate few major changes in community structure in the controls, apart from a loss of some open water specialists (Rhodobacteraceae) that declined in the microcosms.

DOM$_{tot}$, HMW and LMW additions resulted in assemblages of significantly lower taxonomic richness. Distinct species assemblage occurred in the DOM$_{tot}$ compared to the HMW and LMW treatments (PERMANOVA, $P < 0.01$, Fig. 4b), the former dominated by OTUs from a subset of mainly Gammaproteobacteria and Bacteriodetes, accounting for over 94% of all sequences (Fig. 4c, Table S3). All of the OTUs selected for by the DOM additions (with the exception of two Alteromonadales) were also present in the T216 control (seawater) bacterial community.

Bacterioplankton assemblages in the HMW and LMW treatments responded similarly (no difference in NMDS profile, Fig 4b), with significantly higher relative abundance of Bacteroidetes, Flavobacteriaceae and Gammaproteobacteria. All were taxa found in sea ice and underlying water (*49*, *54*), and were able to rapidly utilize the ice-derived DOC and DON. The major Gammaproteobacteria in the enrichments were Alteromonadales, with a

number of different *Colwellia* OTUs enriched. *Colwellia* is a successful polar taxon that produces highly-adapted extracellular enzymes to breakdown organic compounds (*55*). *Colwellia* live within the sea ice matrix (*54*), as well as in the underlying water (Fig. 4c), and our results show that representatives of this genus can rapidly and efficiently grow on the sea-ice HMW and LMW fractions. *Colwellia* taxa from the nearshore Chukchi Sea also grow well on riverine DOM (*42*). The HMW addition stimulated the growth of Flavobacteriaceae, particularly *Polaribacter* and *Tenacibaculum* (including 3 OTUs identified at T0). Bacteriodetes are known degraders of complex organic molecules (*56*) and *Polaribacter* are facultative or obligate psychrophiles present in seawater and ice (*42, 49*), and capable of degrading polymeric organic compounds, including phytoplankton and terrestrial DOM (*42*). Our results support the observation that *Polaribacter* are sentinel taxa for increased organic matter inputs (*42*). *Tenacibaculum* has been isolated from bacterioplankton (*41, 57*) and grows on complex EPS from estuarine diatom biofilms (*56*).

The DOM_{tot} addition resulted in a different community composition than the HMW and LMW treatments (Fig. 4a,b,c), stimulating the growth of *Colwellia* taxa (including OTUs that also grew in the HMW and LMW additions), and particularly a number of *Psychrobium*, *Psychromonas* and *Moritella* (Gammaproteobacteria) OTUs (Fig. 4). *Psychromonas* is a psychrophilic genus found across the Arctic (*58*) that can degrade complex polysaccharides while *Moritella* are linked to fish disease (as are *Tenacibaculum*), degrading amino acid-rich mucus and glycoproteins, possibly permitting growth on the DON-rich compounds present and utilized in the DOM_{tot} addition (Fig. 1b, Table 1).

Sea ice cover in the Arctic Ocean is becoming increasingly seasonal, with an increase in areas of open water and marginal ice zones during the spring-summer months (*3, 4*) and an overall amplification of sea ice-pelagic interactions in extended regions of FYI cover. FYI can support more productive ice algal communities than multiyear ice (*59*). We have shown

that different sea ice DOM fractions stimulate different phylogenetic subsets of the surface water column bacterioplankton community, with increases in cell density and productivity, and changes in species composition, and are utilized at different rates. Our experimental results show that a spectrum of substrates provided by seasonal sea ice melt, from low to high molecular weight and from nitrogen- to sulfur- rich compounds, are selectively utilized by different taxa within the plankton, resulting in changes in the composition of bacterioplankton. While some taxa of Arctic bacterioplankton are able to use a wide range of substrates, some planktonic taxa within the Alphaproteobacteria and Actinobacteria do not readily use sea ice DOM. The preferential utilization of sea ice DOM fractions >10 kDa and >100 kDa by bacterioplankton also has important ramifications for the biogeochemical cycling of organic matter in the Arctic system. These high molecular weight fractions make up the abundant gel-like exopolymeric substances (EPS) that play key ecological roles such as organic matter aggregation (*6*) and the production of atmospherically active bioaerosols (*26*). Implicit to our results is that these EPS fractions are a highly bioavailable carbon source for under ice microbial communities.

Unraveling the significance and repercussions of our results to the Arctic Ocean requires consideration of various factors involved in the cycling of DOM. During our experiment, grazing, DOM production by autotrophic cells, and photodegradation were controlled for, allowing the identification of bacterial responses to sea ice DOM fractions without potential changes in DOM concentrations or composition due to these other factors. Viral activity, responses to inorganic nutrients and low salinity conditions (DOM_{tot} treatment) may have affected net changes in bacterial assemblages over time and between treatments (*60*). Photochemical degradation of DOM under the ice is considered negligible (*61*), though it is probable that photodegradation will increase with increased melt pond coverage and

associated light transmission through the ice cover (*11*), which can also lead to increased under-ice phytoplankton blooms (*11, 62*).

By showing that FYI DOM fractions are efficiently used by sub-groups of surface waters bacterial communities, our results indicate that the continued shift towards a seasonal sea ice regime in the Arctic Ocean, while having only a minor impact on Arctic Ocean DOM inventories, may have a disproportionate impact on DOM remineralization in surface waters. This dual understanding of DOM cycling in the seasonally ice covered Arctic reconciles divergent perspectives on inventories (*63*) and rates (6, 11), both fundamental to constrain ocean-climate models.

Climate change has resulted in FYI already becoming the dominant type of ice in the Arctic Ocean (*3, 4*), with a complete seasonal ice cover predicted to occur over coming decades (*12*). More labile DOM will be released from sea ice to the surface ocean under these future scenarios of sea ice cover in those regions of the Arctic Ocean that will remain ice dominated (*30, 59*). How large areas previously covered by multiyear ice will respond to changes in sea ice biochemistry and seasonal dynamics remains a fundamental question in defining the role of the "new" Arctic in biogeochemical cycles. Earth system models incorporating the role of DOM across the Arctic (*64*) require a mechanistic understanding of the composition and turnover of DOM to constrain biogeochemical fluxes within the ice and at the ice-water interface under future climate scenarios. We propose that sea ice-produced DOM fractions, once released into surface waters, provide ecological niches for taxon-specific bacterial activity. Based on our results, the expansion of FYI and altered temporal and spatial gradients in the release of sea ice-derived DOM fractions, will increase bacterial respiration and modify microbial community structure and dynamics at sea ice-water interfaces, including ice margins. We further propose that these changes will affect the

283 cycling of key elements, and possibly microbial evolutionary pathways, in the warming
284 Arctic Ocean.
285

References

1. Cohen, J. et al. Recent Arctic amplification and extreme mid-latitude weather. *Nature Geoscience* **7**, 627-637 (2014).

2. Stroeve, J. C., Markus, T., Boisvert, L., Miller, J. & Barrett, A. Changes in Arctic melt season and implications for sea ice loss. *Geophys. Res. Lett*. **41**, 1216-1225 (2014).

3. Swart, N. C., Fyfe, J. C., Hawkins, E., Kay, J. E. & Jahn, A. Influence of internal variability on Arctic sea-ice trends. *Nat. Climate Change*, **5**, 86-89 (2015).

4. Perovich, D. K. et al. Sea ice. In Arctic report card (2015), NOAA. 33-40. http://www.arctic.noaa.gov/reportcard

5. Clark, G. F. et al. Light driven tipping points in polar ecosystems. *Glob. Chang. Biol*. **19,** 3749-3761 (2013).

6. Vancoppenolle, M. et al. Role of sea ice in global biogeochemical cycles: emerging views and challenges. *Quat. Sci. Rev*. **79**, 207-230 (2013).

7. Krembs, C. & Deming, J. W. The role of exopolymers in microbial adaptation to sea-ice. In: *Psychrophiles: from biodiversity to biotechnology*, Margesin, R., Schinner, F., Marx, J-C., Gerday, C. Eds. (Springer-Verlag 2008), pp 247-264.

8. Krembs, C. Eicken & H. Deming, J. W. Exopolymer alteration of physical properties of sea ice and implications for ice habitability and biogeochemistry in a warmer Arctic. *Proc. Natl. Acad. Sci. U.S.A.* **108,** 3653-3658 (2011).

9. Underwood, G. J. C. et al. Broad-scale predictability of carbohydrates and exopolymers in Antarctic and Arctic sea ice. *Proc. Natl. Acad. Sci. U.S.A.* **110**, 15734-15739 (2013).

10. Aslam, S. N., Michel, C., Niemi, A. & Underwood, G. J. C. Patterns and drivers of carbohydrate budgets in ice algal assemblages from first year Arctic sea ice. *Limnol. Oceanogr*. **61**, 919-937 (2016).

11. Leu, E. et al. Arctic spring awakening – Steering principles behind the phenology of vernal ice algal blooms. *Prog. Oceanogr.* **139**, 151-170 (2015).

12. AMAP, Snow, Water, Ice and Permafrost. Summary for Policy-makers. Arctic Monitoring and Assessment Programme (AMAP), Oslo, Norway. 20 pp (2017).

13. Bowman, J. S. et al. Microbial community structure of Arctic multiyear sea ice and surface seawater by 454 sequencing of the 16S RNA gene *ISME J.* **6**, 11-20 (2012).

14. Hatam, I., Lange, B., Beckers, J., Haas, C. & Lanoil, B. Bacterial communities from Arctic seasonal sea ice are more compositionally variable than those from multi-year sea ice. *ISME J*. **10**, 2543-2552 (2016).

15. Verdugo, P. Marine microgels. *Ann. Rev. Mar. Sci.* **4**, 375-400 (2012).

16. Benner, R. & Amon, R. M. W. The size-reactivity continuum of major bioelements in the ocean. *Annu. Rev. Mar. Sci.* **7**, 185-205 (2015).

17. Amon, R. M. W., Fitznar, H. P. & Benner, R. Linkages among the bioreactivity, chemical composition, and diagenetic state of marine dissolved organic matter, *Limnol. Oceanogr.* **46**, 287–297 (2001).

18. Riedel, A., Michel, C. & Gosselin, M. Seasonal study of sea-ice exopolymeric substances on the Mackenzie shelf: implications for transport of sea-ice bacteria and algae. *Aquat. Microb. Ecol.* **45**,195-206 (2006).

19. Juhl, A. R., Krembs, C. & Meiners, K. M. Seasonal development and differential retention of ice algae and other organic fractions in first-year Arctic sea ice. *Mar. Ecol. Prog. Ser*. **436**, 1-16 (2011).

20. Smith, R. E. H., Gosselin, M., Kudoh, S., Robineau, B. & Taguchie, S. DOC and its relationship to algae in bottom ice communities. *J. Mar. Syst*. **11,** 71-80. (1997).

21. Michel, C., Riedel, A. & Mundy, C. J. Biological investigation of first-year sea ice near resolute bay, Nunavut, spring to early summer 2001. *Can Data Rep Hydrogr Ocean Sci* **160** vi + 28 pp (2003).

22. Riedel, A, Michel, C. & Gosselin, M. Grazing of large-sized bacteria by sea-ice heterotrophic protists on the Mackenzie shelf during the winter-spring transition. Aquat *Microbiol Ecol* 50: 25-38 (2017)

23. Meiners, K., Brinkmeyer, R., Granskog, M. A. & Lindfors, A. Abundance, size distribution and bacterial colonization of exopolymer particles in Antarctic sea ice (Bellingshausen Sea). *Aquat. Microb. Ecol.* **35**, 283–296 (2004).

24. Niemi, A. Meisterhans, G. & Michel, C. Response of under-ice prokaryotes to experimental sea-ice DOM enrichment. *Aquat. Microb. Ecol.* **73**, 17-28 (2014).

25. Assmy, P. et al. Floating ice-algal aggregates below melting Arctic sea ice. *PLoS ONE* **8**, e76599 (2013).

26. Wilson, T. W. et al. A marine biogenic source of atmospheric ice-nucleating particles. *Nature* **525**, 234-238 (2015).

27. Holding, J. M. et al. Autochthonous and allochthonous contributions of organic carbon to microbial food webs in Svalbard fjords. *Limnol. Oceanogr.* **62,** 1307–1323 (2017).

28. Jørgensen, L., Stedmon, C. A., Kaartokallio, H., Middelboe, M. & Thomas, D. N. Changes in the composition and bioavailability of dissolved organic matter during sea ice formation. *Limnol. Oceanogr*. **60,** 817-830 (2015).

29. Galindo, V. et al. Biological and physical processes influencing sea ice, under-ice algae, and dimethylsulfoniopropionate during spring in the Canadian Arctic Archipelago. *J. Geophys. Res. Oceans,* **119**, doi:10.1002/2013JC009497 (2014).

30. Meiners, K.M. & Michel, C. Dynamics of nutrients, dissolved organic matter and exopolymers in sea ice. In: *Sea Ice*, 3rd Edition, Thomas, D.N. (Ed). Wiley Blackwell, pp 415-432. (2017).

31. Aslam, S. N., Strauss, J., Thomas, D. N., Mock, T. & Underwood, G. J. C. Identifying metabolic pathways for production of extracellular polymeric substances (EPS) by the diatom Fragilariopsis cylindrus inhabiting sea ice. *ISME J.* **12**, 1237-1251 (2018).

32. Sleighter, R. L. & Hatcher, P. G. The application of electrospray ionization coupled to ultrahigh resolution mass spectrometry for the molecular characterization of natural organic matter, *J. Mass Spectr.* **42**, 559-574 (2007).

33. Shen, Y. Fichot, C. G. & Benner, R. Dissolved organic matter composition and bioavailability reflect ecosystem productivity in the Western Arctic Ocean. *Biogeosciences* **9**, 4993-5005 (2012).

34. Michel, C., Ingram, R. G. & Harris, L. R. Variability in oceanographic and ecological processes in the Canadian Arctic Archipelago. *Prog. Oceanogr*. **71,** 379–401 (2006).

35. Niemi, A., Michel, C., Hille, K. & Poulin, M. Protist assemblages in winter sea ice: setting the stage for the spring ice algal bloom. *Polar Biol*., **34,** 1803-1817 (2011).

36. Chin, W., Orellana, M. V. & Verdugo, P. Spontaneous assembly of marine dissolved organic matter into polymer gels. *Nature* **391**, 568–572 (1998).

37. Mundy, C. J., et al. Role of environmental factors on phytoplankton bloom initiation under landfast sea ice in Resolute Passage, Canada. *Mar. Ecol. Prog. Ser*. 497: 38-49 (2014).

38. Elliott, A. et al. Spring production of mycosporine-like amino acids and other UV-absorbing compounds in sea ice-associated algae communities in the Canadian Arctic *Mar. Ecol. Prog. Ser*. **541,** 91–104, (2015).

379 39. Arnosti, C. & Steen, A. Patterns of extracellular enzyme activities and microbial
380 metabolism in an Arctic fjord of Svalbard and in the northern Gulf of Mexico: contrasts in
381 carbon processing by pelagic microbial communities. *Front. Microbiol.* **4**, 1 (2013).
382 40. Steen, A. D. & Arnosti, C. Picky, hungry eaters in the cold: persistent substrate selectivity
383 among polar pelagic microbial communities. *Front. Microbiol.* **5**, 527 (2014).
384 41. Teeling H. et al. Recurring patterns in bacterioplankton dynamics during coastal spring
385 algae blooms *eLife* 5:e11888. (2016) DOI: 10.7554/eLife.11888
386 42. Sipler, R. E. et al. Microbial Community Response to Terrestrially Derived Dissolved
387 Organic Matter in the Coastal Arctic. *Front. Microbiol.* **8**,1018. (2017) doi:
388 10.3389/fmicb.2017.01018
389 43. Ortega-Retuerta, E. et al. Carbon fluxes in the Canadian Arctic: patterns and drivers of
390 bacterial abundance, production and respiration on the Beaufort Sea margin, *Biogeosciences*
391 **9**, 3679–3692 (2012).
392 44. Kirchman, D. L. et al. Standing stocks, production, and respiration of phytoplankton and
393 heterotrophic bacteria in the western Arctic Ocean. *Deep Sea Res Part II Top Stud Oceanogr*
394 **56**, 1237–1248 (2009).
395 45. Arnosti, C. Microbial extracellular enzymes in the marine carbon cycle. *Annu. Rev. Mar.*
396 *Sci.* **3**, 401-425 (2011).
397 46. Troussellier, M., Bouvy, M., Courties, C. & Dupuy, C. Variation of carbon content
398 among bacterial species under starvation conditions. *Aquat. Microb. Ecol.* **13**, 113-119
399 (1997).
400 47. Hansell, D. A. & Carlson, C. A. Dissolved organic matter in the ocean: a controversy
401 stimulates new insights. *Oceanography* **22**, 202-211 (2009).
402 48. Ksionzek, K. B. et al. Dissolved organic sulfur in the ocean: Biogeochemistry of a
403 petagram inventory. *Science*, **354**, 456-459 (2016).

49. Yergeau, E. et al. Metagenomic survey of the taxonomic and functional microbial communities of seawater and sea ice from the Canadian Arctic. *Scientific Reports* **7**, 42242 (2017).

50. Zeng, Y. et al. Phylogenetic diversity of planktonic bacteria in the Chukchi Borderland region in summer. *Acta Oceanol. Sin.* **32**, 66-74 (2013).

51. Pedrós-Alió, C. Potvin, M. & Lovejoy, C. Diversity of planktonic microorganisms in the Arctic Ocean. *Prog. Oceanogr.* **139**, 233-243 (2015).

52. Parada, A. E., Needham, D. M. & Fuhrman, J. A. Every base matters: assessing small subunit rRNA primers for marine microbiomes with mock communities, time series and global field samples. *Environ. Microbiol*. **18**, 1403–1414. (2015).

53. Herlemann, D. P. R. et al. Transitions in bacterial communities along the 2000 km salinity gradient of the Baltic Sea. *ISME J.* **5**, 1571-1579 (2011).

54. Deming, J. W. & Collins, R. E. Sea Ice as a habitat for Bacteria, Archae and viruses. In *Sea Ice*, Thomas, D.N. Ed. 3rd Edition. (Wiley 2017), pp 326-351.

55. Methé, B. A. et al. The psychrophilic lifestyle as revealed by the genome sequence of *Colwellia psychrerythraea* 34H through genomic and proteomic analyses. *Proc. Natl. Acad. Sci. U.S.A.* **102**, 10913-10918 (2005).

56. Bohórquez, J. et al. Different Types of Diatom-Derived Extracellular Polymeric Substances Drive Changes in Heterotrophic Bacterial Communities from Intertidal Sediments. *Front. Microbiol*. **8**, 245 (2017).

57. Frette, L., Jørgensen, N. O., Irming, H. & Kroer, N. *Tenacibaculum skagerrakense* sp. nov., a marine bacterium isolated from the pelagic zone in Skagerrak, Denmark. *Int. J. Syst. Evol. Microbiol.* **54**, 519-24 (2004).

427 58. Groudieva, T., Grote, R. & Antranikian, G. *Psychromonas arctica* sp. nov., a novel
428 psychrotolerant, biofilm-forming bacterium isolated from Spitzbergen. *Int. J. Syst. Evol.*
429 *Microbiol.* **53**, 539-45 (2003).
430 59 Lange, B.A. et al. Comparing Springtime Ice-Algal Chlorophyll a and Physical Properties
431 of Multi-Year and First-Year Sea Ice from the Lincoln Sea. PLoS ONE **10,** e0122418 (2015).
432 60. Thingstad, T. F., Våge, S., Storesund, J. E., Sandaa, R-A. & Giske, J. A theoretical
433 analysis of how strain-specific viruses can control microbial species diversity. *Proc. Natl.*
434 *Acad. Sci. U.S.A.* **111**, 7813–7818 (2014).
435 61. Logvinova, C.L., Frey, K.E., Mann, P.J., Stubbins, A. & Spencer, R.G.M. Assessing the
436 potential impacts of declining Arctic sea ice cover on the photochemical degradation of
437 dissolved organic matter in the Chukchi and Beaufort Seas. *J. Geophys. Res. Biogeosci*., **120**,
438 2326–2344 (2015).
439 62. Horvat, C. et al. The frequency and extent of sub-ice phytoplankton blooms in the Arctic
440 Ocean. *Sci. Adv.* **3**, e1601191 (2017).
441 63. Anderson, L. G., & Amon, R. M. W. DOM in the Arctic Ocean in: *Biogeochemistry of*
442 *Marine Dissolved Organic Matter*, Hansell D. A. & Carlson C. A. Eds. (Academic Press
443 Boston, MA), 2nd Edn. pp. 609–633. (2015).
444 64. Elliot, S. et al. Strategies for the simulation of sea ice organic chemistry: Arctic tests and
445 development: *Geosciences* **7**, 52 (2017).

446

447 *Correspondence and requests for materials to gjcu@essex.ac.uk

448 **Acknowledgments:**
449 GJCU was funded by grants NE/D00681/1 and NE/E016251/1 from the U.K. Natural
450 Environment Research Council. CM received financial support from the Natural Sciences and
451 Engineering Council of Canada (Individual Discovery Grant), the International Governance

Strategy (Fisheries and Oceans Canada), and the Polar Continental Shelf Program (Natural Resources Canada) for the project Sea Ice BIOTA (Biological Impacts Of Trends in the Arctic). GM received a Visiting Fellowship in Canadian Government Laboratory from the Natural Sciences and Engineering Council of Canada. C. Burau is acknowledged for performing solid-phase extraction. We thank S. Duerksen, D. Jordan, M. Poulin, and A. Reppchen for their help in the field and laboratory. We also greatly appreciate the support from the Resolute Bay Hunters and Trappers Association and the excellent logistical support from the Polar Continental Shelf Program in Resolute, Nunavut.

Author Contributions

GJCU, CM and AN designed the study, GJCU, CM and GM conducted the experiments, MW carried out FT-ICR-MS analysis, GJCU, CM, CB, GM, AW, BPK, AJD analyzed the data, and GJCU, CM, BPK and AJD wrote the manuscript.

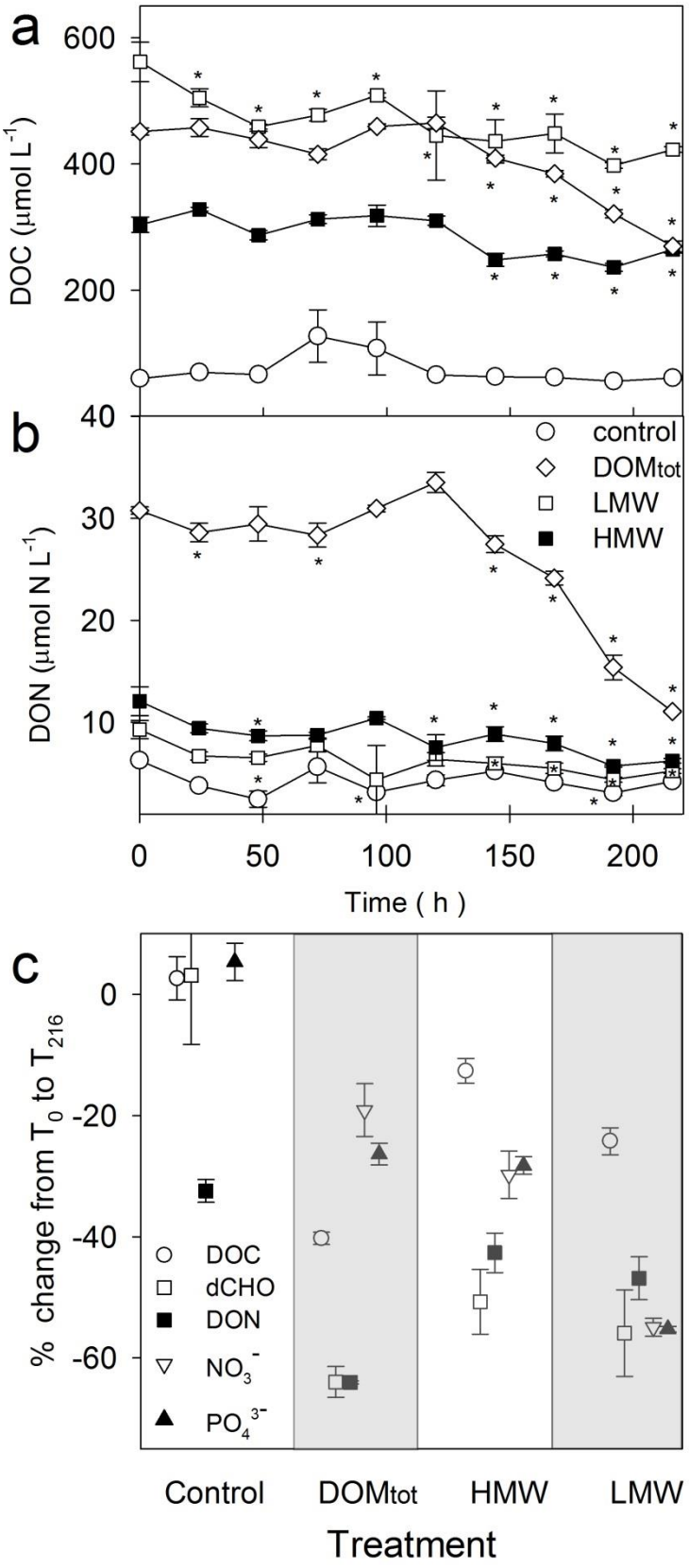
a
b
c
DOC (µmol L-1)
DON (µmol N L-1)
control
DOMtot
LMW
HMW
Time (h)
% change from T0 to T216
DOC
dCHO
DON
NO3-
PO43-
Control
DOMtot
HMW
LMW
Treatment

467 .
468

Fig. 1. Changes in concentrations of dissolved organic and inorganic components during experiments of Arctic under-ice surface water enriched with three sea ice derived organic matter fractions (DOM, LMW and HMW). (a) dissolved organic carbon (DOC), (b) dissolved organic nitrogen (DON) concentrations, (c) percent utilization of dissolved organic and inorganic C, N, and P components (comparing T_0 to T_{216} h). Symbols, mean ± standard error, n = 3. * indicate samples significantly different (ANOVA $P < 0.01$ or less) from T0 concentration.

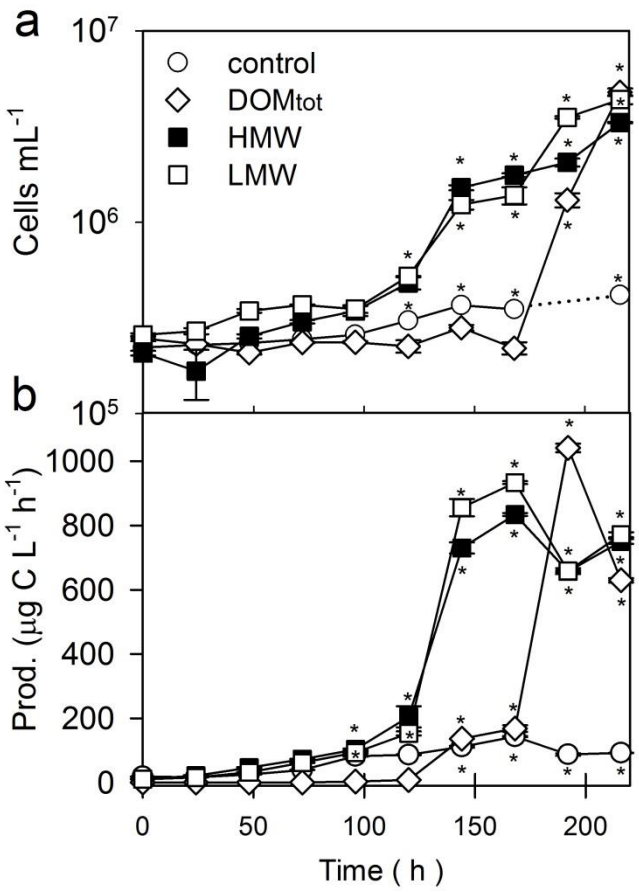

Fig. 2. Changes in bacterial cell density and productivity over 9 days (216 h) in Arctic under-ice surface water enriched with three sea ice derived organic matter fractions (DOM, LMW and HMW). (a) bacterial cell density, (b) bacterial production. Symbols mean ± standard error, n = 3. * indicate samples significantly different (ANOVA $P < 0.001$ or less) from T0 values.

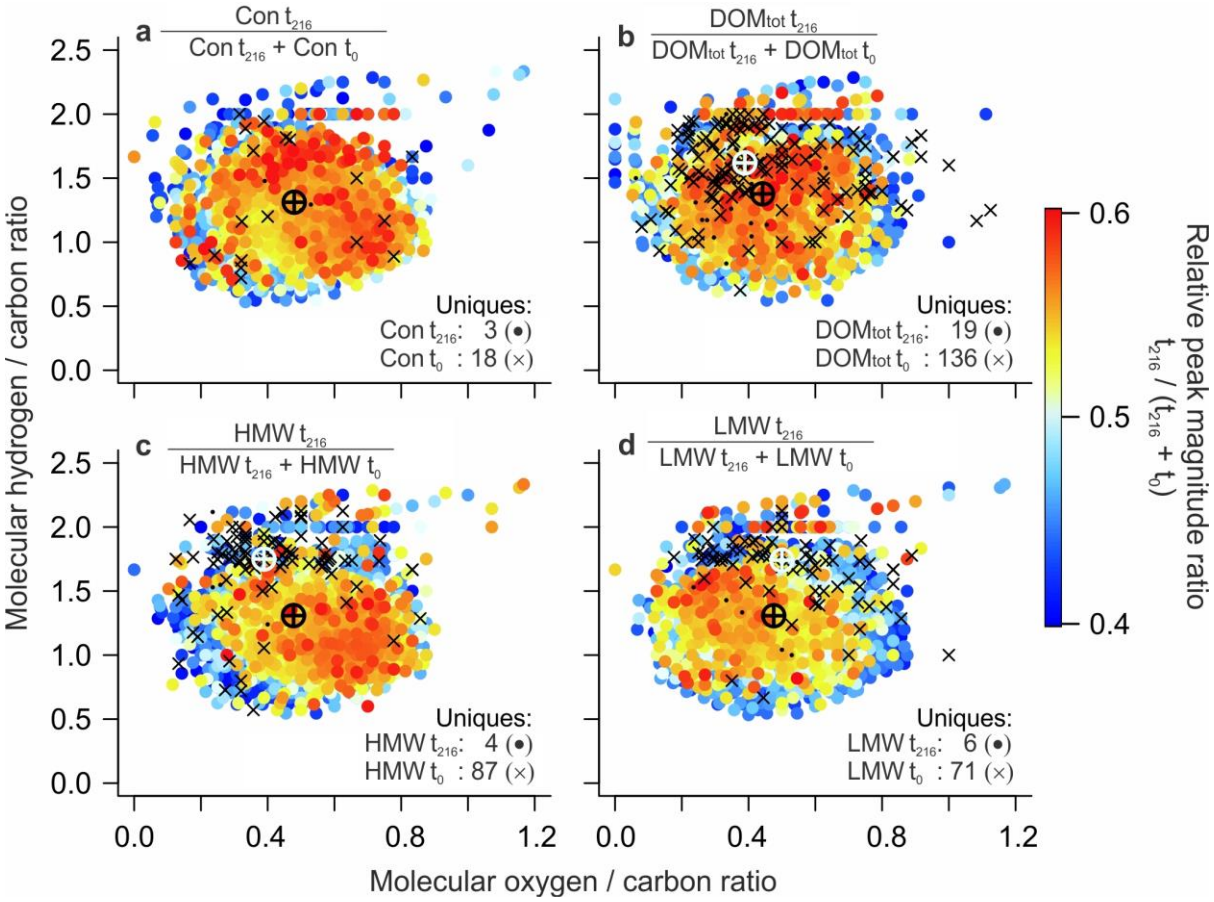

Fig. 3. Element ratio (van Krevelen) plots of molecular formulas determined by FT-ICR-MS in control and three organic matter enriched treatments over a 216 h incubation. (a) control, (b) DOMtot (c) HMW and (d) LMW treatments. Each dot represents at least one detected molecular formula represented as the molecular oxygen/carbon and hydrogen/carbon ratio. Colours represent changes in relative peak magnitude ratios over incubation time. Higher values (in red) and the number of unique formulas in controls (crosses) and after 216 days (dots) are indicated. The average elemental compositions for all (black marker) and unique molecular formulas in the control (white marker) are also shown.

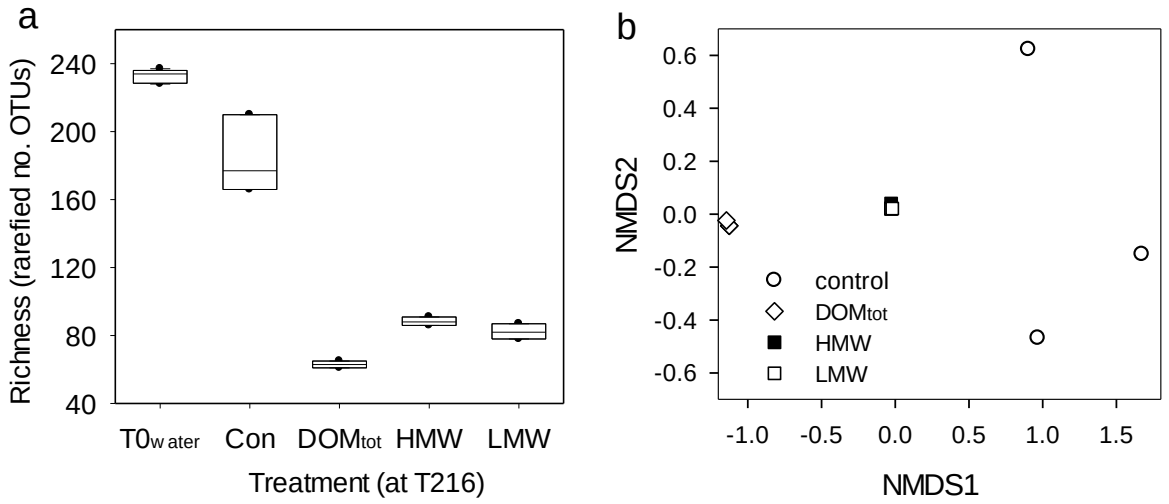

c

Taxon	T0 water	Control.a	Control.b	Control.c	DOM^{tot}.a	DOM^{tot}.b	DOM^{tot}.c	HWM.a	HMW.b	HMW.c	LMW.a	LMW.b	LMW.c
Acidobacteria													
Acidobacteria_Gp6		1.5	4.1	3.0	0.0	0.0	0.0	0.0	0.0	0.0	0.0	0.0	0.1
Actinobacteria *	1.0												
Cellulomonadaceae; *Cellulomonas*		2.2	3.4	2.5	0.0	0.2	0.1	0.0	0.1	0.1	0.0	0.1	0.1
Bacteroidetes													
Flavobacteriaceae; *Polaribacter* [1]	1.3	0.0	0.0	0.0	0.0	0.0	0.0	0.7	0.3	0.2	0.2	0.5	0.3
Flavobacteriaceae; *Polaribacter* [2]	0.6	0.4	0.1	0.1	0.0	0.1	0.1	2.7	2.8	2.7	2.5	3.8	3.6
Flavobacteriaceae; *Tenacibaculum* [1]	1.0	0.4	0.1	0.0	0.0	0.0	0.0	0.4	0.8	0.6	0.5	0.3	0.5
Flavobacteriaceae; *Tenacibaculum* [2]		0.0	0.1	0.0	0.0	0.0	0.0	0.5	0.7	0.6	0.8	1.0	0.7
Cytophagaceae; *Adhaeribacter*		1.3	1.3	1.9	0.0	0.1	0.2	0.0	0.0	0.1	0.6	0.1	0.1
Firmicutes													
Bacillaceae 1; *Bacillus*		2.8	3.4	8.3	0.6	0.5	1.3	0.9	0.5	0.3	0.3	0.2	0.3
Alphaproteobacteria *	2.5												
Rickettsiales; Pelagibacteraceae	11.3	12.3	23.4	16.7	0.0	0.0	0.0	0.1	0.0	0.0	0.1	0.0	0.0
		1.1	1.9	0.9	0.0	0.0	0.0	0.0	0.0	0.0	0.0	0.0	0.0
Rhizobiales; Hyphomicrobiaceae; *Devosia*	0.1	1.3	7.2	7.6	0.3	0.0	0.3	0.1	0.1	0.0	0.1	0.1	0.1
Rhizobiales; Methylobacteriaceae		3.0	6.5	7.4	0.0	0.1	0.1	0.1	0.0	0.1	0.2	0.1	0.0
Rhodospirillales; *Roseomonas*		2.2	1.5	7.9	0.1	0.1	0.1	0.4	0.0	0.0	0.1	0.0	0.0
Rhodobacterales; Rhodobacteraceae *	2.4	0.0	0.0	0.0	0.0	0.0	0.0	0.0	0.0	0.0	0.0	0.0	0.0
Betaproteobacteria; Burkholderiales *	0.1												
Oxalicibacterium		0.9	0.8	2.8	0.0	0.0	0.0	0.1	0.1	0.0	0.0	0.0	0.1
Gammaproteobacteria; Alteromonadales *	14.9												
denovo15318		0.0	0.0	0.0	0.1	0.1	0.0	0.2	0.3	0.1	0.2	0.3	0.2
Psychorium		0.1	0.2	0.1	3.0	3.0	3.3	1.1	1.0	0.7	2.1	1.7	1.3
Colwellia [1]	0.0	0.0	0.3	0.1	2.5	2.2	2.2	1.5	1.4	1.9	2.2	2.1	2.2
Colwellia [2]		30.5	10.7	9.5	0.4	0.0	0.4	22.4	21.9	18.5	18.9	17.1	22.9
Colwellia [3]		0.8	2.0	0.6	2.7	3.7	3.9	8.2	7.9	6.2	5.3	4.4	8.1
Colwellia [4]	0.0	0.1	0.2	0.0	0.0	0.4	0.0	0.0	0.1	0.0	0.1	0.0	0.0
Colwellia [5]		0.4	2.1	0.2	7.8	7.1	7.8	22.2	28.2	25.0	28.4	22.8	30.5
Thalassomonas	0.0	0.0	0.0	0.0	0.2	0.1	0.2	0.4	0.2	0.2	0.3	0.6	0.2
Moritellaceae; *Moritella*	2.2	2.2	1.6	1.5	63.2	67.1	67.6	27.4	21.4	30.9	26.2	32.4	16.6
Psychromonadaceae; *Psychromonas*	0.1	0.1	0.3	0.1	14.6	10.5	8.3	1.3	1.1	1.5	2.5	3.5	2.6
Gammaproteobacteria; Oceanospirillales *	29.6												
denovo19004	0.0	12.3	3.1	2.4	0.0	0.0	0.0	3.7	3.8	2.9	2.3	2.0	3.2
denovo22973		0.5	0.2	0.3	0.2	0.1	0.1	0.1	0.3	0.3	0.4	0.7	0.4
Oleispira		0.4	0.1	0.1	1.1	1.2	0.7	0.5	0.6	0.7	0.8	0.5	0.5
SUM % of total OTU	**67**	**77**	**75**	**74**	**97**	**97**	**97**	**95**	**94**	**94**	**95**	**94**	**94**
total OTU count	*38922*	*2481*	*2523*	*3054*	*4507*	*4735*	*4475*	*3617*	*3554*	*3510*	*3705*	*3863*	*3289*

Fig. 4. Changes in bacterioplankton taxonomic richness and diversity between under ice seawater (T0water) and with addition of three sea-ice derived organic carbon fractions (DOMtot, HMW, LMW) after 216 hours incubation. (a) rarefied taxonomic richness (OTU)

of under-ice bacterial assemblages from 16S rRNA operational taxonomic units (OTU) at T0 and T216 h, (b) non-metric multidimensional scaling (NMDS) of taxonomic composition at T216 h, note that HMW and LMW data points overlap, PERMANOVA, $F_{3,11} = 23.43$, $R^2 = 0.92$,P = 0002, (c) heat map (% relative abundance) of bacterial operational taxonomic units (OTU) from 454 sequencing of 16S rRNA at T216, and in T0 (from Ion PGM 16S rRNA sequencing) underlying seawater (OTU listed if contributing at least 0.15% of the total sample). Warm colours indicate greater contribution to overall community. OTU sorted by taxonomic groups and species affiliation. * indicates OTUs identified only to family or higher taxonomic level in T0 water. SUM % of population = overall contribution of taxa listed to the total OTU count of sample, total OTU sample size given. Symbols represent mean ± standard error, n = 3 (a, b), or individual triplicate scores, except T0 where n = 5 (a) and pooled overall community composition (c).

Table 1. Substrate utilization during experiments of Arctic under-ice surface water enriched with three sea-ice derived organic matter fractions. Apparent utilization (substrate used per net bacterial cell growth, see methods) for DOC, dCHO, non-dCHO dissolved organic carbon, DN, DON, NO_3^- and PO_4^{3-} are all significant at $P < 0.001$, except * denotes $P < 0.05$. - = low growth rates in controls prevented calculation of utilization quota. ns = calculated utilization value not significantly different from zero. Intensity-weighted average elemental H:C, C:N and C:S ratios determined by FT-ICR-MS in the < 600 Da molecular fraction and number of completely utilized or transformed organic compounds (CUC), including those containing N and S, at the end of the 216h experimental period are also shown. Values represent the mean and, in italics, standard error, from triplicate experiments.

Variable / Treatment	Apparent utilization (femtomol C or N bacterial cell^{-1})							Elemental ratio in < 600 Da fraction			Number of CUC.		
	DOC	dCHO	non dCHO	DN	DON	NO_3^-	PO_4^{3-}	H:C	C:N	C:S	Total	N	S
Control	–	–	–	–	–	–	–	1.311 *0.058*	50 *2*	208 *29*	18	4	14
DOM_{tot}	38.13 *4.9*	20.7 *2.9*	17.5 *4.8*	4.9 *0.5*	4.22 *0.54*	0.67 *0.12*	0.24 *0.03*	1.374 *0.009*	81 *12*	176 *15*	136	78	48
HMW	18.53 *8.41*	9.8 *2.5*	ns	1.6 *0.3*	0.77* *0.34*	0.85 *0.12*	0.13 *0.01*	1.298 *0.008*	56 *5*	211 *61*	87	44	28
LMW	22.29 *7.09*	7.3 *1.9*	15.0* *7.6*	1.9 *0.2*	0.98 *0.21*	0.91 *0.11*	0.17 *0.01*	1.304 *0.009*	55 *4*	199 *36*	71	41	21

Methods

Surface water and first-year ice (FYI) sea ice cores were collected on May 1st 2012 at a first-year sea-ice station (74.75° N, 95.50° W) located ca. 2 km offshore in Resolute Passage, Canadian Arctic Archipelago (Nunavut). Resolute Passage is typically covered by landfast FYI from late November to the beginning of July. Twenty six (26) sea-ice cores were collected using a manual ice corer (Mark II coring system, 9 cm internal diameter, Kovacs Enterprises). The bottom 3 cm sections of the cores, where most of the sea-ice biomass is found (*29*), were cut with a clean stainless steel saw and stored in sterile WhirlPak bags. Surface water (60 L) was collected using a pump installed on an underice arm, reaching out 1 m away from the hole. The water collected from the ice interface was free of ice (initial flow with potential presence of ice was left out). The acid-washed Nalgene container in which the water was transferred was rinsed three times with the sample prior to filling. The sea ice and surface water samples were transported back to the shore laboratory where they were kept in the dark at near 0°C temperatures until the beginning of the experiments. Experiments began the day following sample collection to allow the ice samples to melt slowly overnight. Experiments and sample processing were conducted at the Polar Continental Shelf Program laboratory facilities, Resolute Bay, Nunavut.

Starting conditions.

Sea ice core sections were melted within 24 h of collection in sterile whirlpak bag at 4 ^{o}C temperature in darkness *without* the addition of filtered sea water. Melted material was filtered through precombusted (450 ^{o}C for 24 h) Whatmann GF/F and pooled, giving a total volume of 3225 mL, and stored at 4 ^{o}C.

Four fully replicated treatments were established, with 30 sterile Whirlpack bags each filled with 300 mL of starting condition media for each of the four treatments. Control treatments consisted of under ice seawater filtered through a 3 µm filter to remove larger

561 protists and grazers. DOM_{tot}-enrichments consisted of GF/F filtered DOM obtained from
562 melted bottom ice core sections, added to filtered (3 µm filter) under ice seawater (ratio
563 DOM:seawater 1:5.3), giving a final DOC concentration of 451 µmol C L^{-1} (Table S1). Two
564 molecular weight-fractionated DOM enrichments (a high molecular weight –enhanced DOM
565 fraction (HMW) retained above an 100 kDa filter (known to be rich in diatom EPS larger
566 than 100 kDa); and (iii) and an intermediate lower molecular weight (LMW) EPS-rich DOM
567 fraction between retained between 10 kDa and 100 kDa filters), were established by
568 sequentially filtering 1715 mL of the melted ice-core DOM extract through 100 kDa and 10
569 kDa molecular filters (Amicon Millipore Ltd., Watford U.K.) to separate the polydisperse
570 DOM pool into two molecular weight fractions. The filter sizes correspond to those used to
571 investigate TEP formation in seawater (*65*), and in studies of diatom and algal EPS
572 investigations, with the 10-100 kDa providing a separation between the lower and higher
573 molecular weight colloidal exudates produced by polar algae (*16, 66, 67*).
574 The HMW fraction contained the dissolved organic constituents retained in a final
575 volume of 195 mL above a 100 kDa molecular filter (from 1715 mL filtered). This 100 kDa –
576 enriched fraction was added to 9.3 L of (3 µm filtered) under ice seawater to give a final
577 DOC concentration of 304 µmol C L^{-1} (Table 1). The 1520 mL of 100 kDa filtrate was
578 reduced to a final volume of 215 mL above a 10 kDa Amicon filter, and this fraction (LMW,
579 <100 kDa and >10 kDa molecular weight) was added to 9.3 L filtered under ice seawater to
580 give a final DOC concentration of 562 µmol C L^{-1} (Table 1). The Whirlpak bags were sealed
581 and placed in a chilled incubator facility, and maintained in darkness at an average
582 temperature of -1.72 ºC ± 0.021 ºC (Hobo data loggers) over a period of 216 h. Bags were
583 checked and rotated daily. Every 24 h, three replicate bags from each treatment and controls
584 were sampled. Each bag was manually mixed and samples taken to measure the following
585 variables: At each experimental time, sub-samples were collected and analyzed for

prokaryotic abundance and production, dissolved organic carbon (DOC), dissolved nitrogen (DN), inorganic nutrients (PO_4^{3-}, $SiOH_4$, NO_3^-+NO_2^-), and carbohydrate concentrations.

Analytical water chemistry

Surface water and sea-ice salinity was measured with a salinometer probe (Portsal 8410A, Technel). 13 mL of sample was taken for nutrient analysis. Filtered samples (precombusted Whatman GF/F filters) were stored at −80°C for later determination of nitrate (NO_3^-), nitrite (NO_2^-) phosphate (PO_4^{3-}) and $Si(OH)_4$ concentrations using a SmartChem discrete analyzer (Westco Scientific Instruments). Nutrient chemistries were adapted from (*68*).

25 mL of water was filtered through pre-combusted (450°C for 5 h) GF/F filters, with first 5 mL dispensed with as a rinse, and 20 mL stored in pre-combusted acid-washed amber bottles at 4 ºC in fridge after being acidified with 50% H_3PO_4. DOC and DN were measured on a Shimadzu TOC-VCPH analyzer with an ASI-V auto sampler and TNM-1 Total Nitrogen module, using high-temperature catalytic combustion (*69*). The analyses were systematically checked against consensus reference material, i.e. deep seawater reference (DSR), from the Hansell's Certified Reference Materials (CRM) program. The remaining 250 mL was GF/F filtered into acid-washed plastic bottles and frozen at -20 ºC for subsequent carbohydrate and EPS, and FT-ICR-MS analysis.

Dissolved carbohydrate (dCHO)

Filtrates were used for dissolved carbohydrates (dCHO), a subsample (0.4 mL) of GF/F filtrate was used to determine total dissolved carbohydrate concentration ($dCHO_{TOTAL}$) using a modified phenol sulphuric acid assay (*70*) as described by (*10*). The modified Dubois assay measures a range of neutral sugars (hexoses and pentoses), as well as acidic carbohydrates (uronic acids) (*70*). It shows different sensitivities to different constituents, but is a stable assay, and widely used in microbial ecology studies of EPS and microbial

polysaccharides, (*8, 10, 66, 71, 72*). To estimate EPS concentrations, a 3 mL subsample of GF/F filtrate was subject to a 70% v/v ethanol precipitation for 24 h at 4 ºC, followed by centrifugation to isolate the EPS pellet. The precipitation of EPS using an alcohol solvent is an established polysaccharide chemistry technique (*71, 73*). The pellet was resuspended in distilled water and analyzed using the phenol sulphuric acid assay (*10*). Glucose was used as a standard, with standard curves modified with NaCl where necessary to correspond to the salinity of the fraction being measured. Carbohydrate concentrations calculated as glucose-carbon-equivalents and converted to µmol C L^{-1}.

Ultrahigh resolution mass spectrometry (FT-ICR-MS) and data evaluation

Prior to FT-ICR-MS analysis, 100 mL aliquots of each sample were desalted (dialysis at 8 kDa, 24 h in 1 L) and lyophilized. Since remnants of salt prevented electrospray ionization, the dried samples were redissolved in 15 mL ultrapure water (ultrasonification for 15 min). 10 mL aliquots of the redissolved sample were acidified to pH2 (ultrapure HCl, Merck) and solid-phase extracted (PPL adsorber, 200 mg cartridge, Agilent, Lot : 6211763-04; (*74*). FT-ICR-MS analyses were carried out as described previously (*75*). Prior to analysis, DOM extracts were diluted with methanol:water (1:1, v/v). Samples were ionized by electrospray ionization (ESI, Apollo II electrospray ionization source, Bruker Daltonik, Bremen, Germany) in negative mode at an infusion flow rate of 120 µL h^{-1} on a FT-ICR mass spectrometer (SolariX, Bruker Daltonik, Bremen, Germany) equipped with a 12 T refrigerated actively shielded superconducting magnet (Bruker Biospin, Wissembourg, France). 300 scans were added to one mass spectrum. The magnitude threshold for the peak detection was set to a signal to noise ratio of ≥4. Mass spectra were recalibrated internally with compounds, which were repeatedly identified in marine DOM samples (*69*); m/z: 247.06120, 297.13436, 327.14493, 369.15549, 397.15041, 439.16097, 483.18719,

551.24979, 595.23962). The average mass error of the detected compounds was below 50 ppb.

All ions were singly charged as confirmed by the spacing of the related $^{12}C_n$ and $^{13}C_1C_{n-1}$ mass peaks. The spectra were evaluated in the mass range of 200–600 m/z. The base peak in this mass range was defined as 100%, and relative intensities for all other peaks were calculated accordingly. For the process of formula assignment only peaks with a relative intensity between 1-100% were considered. Molecular formulas were calculated from m/z values allowing for elemental combinations $^{12}C_{0-\infty}{}^{13}C_{0-1}{}^{1}H_{0-\infty}{}^{14}N_{0-3}{}^{16}O_{0-\infty}{}^{32}S_{0-2}{}^{34}S_{0-1}$ and a mass accuracy threshold of $|\Delta m| \leq 0.2$ ppm. The double bond equivalent (DBE = 1 + ½(2C – H + N)) of a valid neutral formula had to be an integer value ≥0 and <=20 and the "nitrogen-rule" was applied. Combinations of N_2S_2 (n=614) and N_3S_2 (n=19) were excluded because of a higher average mass error compared to all other elemental combinations. Formulas that were detected in a process blank (PPL extraction of ultrapure water) or in the list of potential surfactants (*76*), as well as formulas containing a ^{13}C or ^{34}S isotope and did not correspond to a parent formula (^{12}C, ^{32}S) were also removed from the dataset. The final dataset contained 95,434 identified molecular formulas. Intensity weighted average (wa) molecular masses and element ratios were calculated based on normalized peak magnitudes. It should be noted that the elemental ratios determined by FT-ICR-MS differ from bulk ratios due to differences in compound specific ionization efficiencies in electrospray ionization. For comparison of treatments the average peak magnitude for each molecular formula within a treatment was calculated (n=3). The evaluation of unique molecular formulas using van Krevelen diagrams was performed for only those formulas which occurred in either all or none of the three samples of a treatment.

Bacterial abundance and productivity

659 The abundance of bacteria was determined by flow cytometry. Duplicate 4 mL
660 subsamples were fixed with glutaraldehyde Grade I (0.5% final concentration; Sigma) in the
661 dark at 4°C for 30 min, and then frozen at -80 °C until analysis. Bacteria samples were
662 stained with SYBR Green I (Invitrogen) and counted with an Epics Altra flow cytometer
663 (Beckman Coulter) fitted with a 488 nm laser operated at 18 mW (*24*). The green
664 fluorescence of nucleic acid-bound SYBR Green I was measured at 525 +/-5 nm. Cytograms
665 obtained were analyzed using Expo32 v1.2b software (Beckman Coulter). The addition of
666 DOM increased the background fluorescence of the samples due to non-specific binding of
667 SYBR Green I to DOM and EPS. Bacteria could not be discriminated from this added
668 fluorescence using the usual approach where bacterial populations are identified on a side
669 scatter vs. green fluorescence scatterplot (*77, 78*). Because of the shift in emission
670 wavelengths upon binding of SYBR Green I to DNA (*79*), it was nevertheless possible to
671 discriminate bacteria from background fluorescence. On a scatterplot of green vs. red
672 fluorescence (measured at 610 nm/BP 20 nm), bacteria stained with SYBR Green fell on a
673 narrow diagonal while DOM and EPS had a higher red fluorescence for a given green
674 fluorescence intensity. Using this approach, bacterial abundance was practically identical in
675 all treatments at T0 (see Fig 2a), when the influence of added DOM and TEP was largest.
676 Bacterial production was measured from the incorporation rates of the tritiated (^{3}H-)
677 amino acid leucine, according to (*80*). This method measures protein production in both
678 bacteria and archaea (*81*), therein referred to as bacterioplankton. Triplicate 1.2 mL
679 subsamples and two controls were inoculated with 3H-leucine (specific activity: 60 Ci
680 mmol^{-1}; final concentration 10 nM). The controls were immediately spiked with 50%
681 trichloroacetic acid (TCA, 5% final concentration). All five vials (measurement and controls)
682 were incubated in the dark at 4 °C for 4 h. At the end of the incubation, TCA (5% final
683 concentration) was added to the vials and samples were frozen at −80 °C until final analysis

684 in our main laboratory. Analyses were performed within 2 months of sample collection. The
685 thawed samples centrifuged at 14000 rpm for 10 min. The supernatant was removed and
686 pellets were rinsed with 1 mL of TCA (5% final concentration). The TCA was removed after
687 a second centrifugation, followed by a third centrifugation. Scintillation cocktail (Ecolume,
688 MP Biomedicals, Santa Ana, CA, USA) was added to the vials, and bacterial cells were
689 resuspended by vortex mixing. ^{3}H-Leucine incorporation was measured using a liquid
690 scintillation counter (TRI-CARB 2100 TR, Packard Bio- Science, Meriden, CT, USA) after
691 48 h of incubation in the dark at 4 °C.
692 Cell-normalized apparent substrate utilization quotas (as femtomols C or N per cell)
693 were calculated from linear regressions between the declining concentrations of substrate and
694 increasing bacterial cell numbers (Table 1) in the three addition treatments. Because there
695 was no significant growth in the controls, no significant regressions could be derived.
696
697 *Bacterioplankton community analysis*
698 The composition of the bacterial community at the beginning of the experiment (T0) was
699 determined by (*82*), on the identical water samples used to set up this experiment. Partial 16S
700 ribosomal (rRNA) gene amplicons were generated using the universal primers F343 (5'-TAC
701 GGR AGG CAG CAG-3') and R534 (5-ATT ACC GCG GCT GCT GGC-3'). Sequencing
702 was performed on an Ion Torrent personal genome machine (PGM) using the Ion 314 chip
703 and the Ion PGM Sequencing 200 kitV2 (Life Technologies) following the manufacturer's
704 instructions. For full details see (*82*).
705 The composition of the bacterial community at the end of the experiment was
706 assessed from 250 mL of sample, from a parallel set of identical treatment bags (n =3),
707 filtered through sterile 0.22 µm Millipore Durapore filters, frozen at -80 °C immediately after
708 filtering, following the methods in (*56*). DNA was extracted from the frozen filters using the
709 MoBio PowerSoil DNA isolation kit using the manufacturer's protocol. 16S rRNA gene

libraries were constructed from these DNA extracts. The sequences of the primers that were specific for bacterial 16S rRNA genes were: Bakt_341F (5´-CCTACGGGNGGCWGCAG-3´ and Bakt_805R (5´-ACHVGGGTATCTAATCC-3´) (*49*). GS FLX Titanium adaptors were at the 5´-end of the Bakt primers: adaptor A for the forward primer (5'-CGTATCGCCTCCCTCGCGCCATCAG-3´) and B for the reverse primer (5'-CTATGCGCCTTGCCAGCCCGCTCAG-3´). Sample-specific 10 bp barcodes were located between the B adaptor and Bakt_805R.

Analysis of pyrosequence data

Sequences were analyzed using the QIIME pipeline and associated modules (*83*). Pyrosequencing data were fully denoised using AmpliconNoise (*84*). Sequences were removed if they: had errors in the 10-bp barcodes and taxon-specific primers, were <450 bp long, had low quality scores (<25) and ≥7 bp homopolymer inserts. Pyrosequences were clustered into operational taxonomic units (OTUs) at the 95% similarity level using USearch and the associated *de-novo* chimera checker (*85*) was used to detect and remove chimeras and OTUs represented by fewer than four sequences across all samples. Representative sequences from each OTU were assigned to a taxonomic group using the Ribosomal Database Project (RDP) classifier algorithm (*86*) version 9, and using a 95% similarity cut off. 80% of raw pyrosequencing read passed our quality filtering and denoising, providing 43,697 sequences from 661 different OTUs. Sequence data are available in the European Bioinformatics institute, http://www.ebi.ac.uk under accession number PRJEB20754 (fastq file names correspond to sample identities).

To compare the T0 and T216 data OTUs captured from T216 (as described above) were used as a custom database against which T0 OTUs were picked using VSEARCH (*87*). T0 data were already denoised and quality filtered (see *82*), but checks for chimeric sequences were included in the new analysis, although none were detected. This approach

provides an ideal solution to combine the two datasets from different sequencing technologies as the resultant amplicon are directly compared, and in this case start within 2bp of each other on the forward primers thus covering the same region of the 16S rRNA gene. Sequences classified as unidentified Bacteria were maintained across datasets, but cyanobacterial plastid sequences were removed, as we were focusing on the heterotrophic bacteria. Amplicon data were normalized via rarefaction before comparing alpha (taxonomic richness) and beta (NMDS analysis based on Bray-Curtis distances) diversity measurements between samples.

Statistical analysis

Differences between treatments and over time were tested using one-way and two-way ANOVA with Tukey post hoc tests, using Minitab v.13.3 (Minitab Inc). Data were tested for normality and homogeneity of variances and log transformation was done on data deviating from these assumptions. Comparison of changes in taxonomic composition were conducted ANOVA, adjusting P-values to accommodate multiple testing. The molecular similarity between treatments (FT-ICR data) was assessed by applying cluster analyses based on untransformed normalized peak magnitudes and Bray Curtis similarity (*88*) and (Software: "R" and Primer, Version 6). All statistical differences mentioned in the paper are significant at $P < 0.05$ or less.

Data Availability

Experimental http://dx.doi.org/10.5526/ERDR-00000072 and FT-ICR-MS data (https://dx.doi.org/10.5526/ERDR-00000084) are available from the University of Essex data repository. Sequence data are archived at the European Bioinformatics institute, http://www.ebi.ac.uk under accession number PRJEB20754.

References

65. Zhou, J., Mopper, K. & Passow, U. The role of surface active carbohydrates in the formation of transparent exopolymer particles by bubble adsorption of seawater. *Limnol. Oceanogr*. **43**, 1860-1871 (1998).

66. Underwood, G. J. C., Fietz, S., Papadimitriou, S., Thomas, D. N. & Dieckmann G. S. Distribution and composition of dissolved Extracellular Polymeric Substances (EPS) in Antarctic Sea Ice. *Mar. Ecol. Prog. Ser.* **404**, 1–19 (2010).

67. Norman, L. et al. The role of bacterial and algal exopolymeric substances in iron chemistry. *Mar. Chem.* **186,** (2015). DOI: 10.1016/j.marchem.2015.03.015

68. Grasshoff, K., Kremling, K. & Ehrhardt, M. Eds. *Methods of seawater analysis*, 3rd edn. (Wiley) (1999).

69. Knap, A. Michaels, A. Close, A., Ducklow, H. & Dickson, A. *Protocols for the Joint Global Ocean Flux Study (JGOFS) core measurements*. JGOFS report no. 19, reprint of the IOC manuals and guides no. 29, UNESCO 1994 (1996).

70. Dubois, M., Gilles, K. A., Hamilton, J. K., Rebers, P. A. & Smith, F. Colorimetric method for determination of sugars and related substances. *Anal. Chem*. **28**, 350-56 (1956).

71. Decho, A. W. Microbial exopolymer secretions in ocean environments: their role(s) in food webs and marine processes. *Oceanogr Mar Biol Annu Rev* **28,** 73-153 (1990).

72. Herborg, L.-M., Thomas, D. N., Kennedy, H., Haas, C. & Dieckmann, C. Dissolved carbohydrates in Antarctic sea ice. *Antarct Sci* **13**,119-125 (2001).

73. Sutherland, I. Biofilm exopolysaccharides: a strong and sticky framework. *Microbiology* **147**, 3-9 (2001).

74. Dittmar, T., Koch, B. P., Hertkorn, N. & Kattner, G. A simple and efficient method for the solid-phase extraction of dissolved organic matter (SPE-DOM) from seawater, *Limnol. Oceanogr. Meth*. **6**, 230-235 (2008).

786 75. Koch, B. P., Kattner, G., Witt, M. & Passow, U. Molecular insights into the microbial
787 formation of marine dissolved organic matter: Recalcitrant or labile? *Biogeosciences,* **11**,
788 4173 - 4190 (2014).
789 76. Lechtenfeld, O. J. et al. The influence of salinity on the molecular and optical properties
790 of surface microlayers in a karstic estuary, *Mar. Chem*. **150**, 25-38 (2013).
791 77. Marie D., Partensky F., Jacquet S. & Vaulot, D. Enumeration and cell cycle analysis of
792 natural populations of marine picoplankton by flow cytometry using the nucleic acid stain
793 SYBR Green I. *Appl. Env. Microbiol*. **63**, 186-193 (1997).
794 78. Gasol, J. M., Zweifel, U. L., Peters, F., Fuhrman, J. A. & Hagström, Å. Significance of
795 size and nucleic acid content heterogeneity as measured by flow cytometry in natural
796 planktonic bacteria. *Appl. Environ. Microbiol.* **65**, 4475-4483 (1999).
797 79. Cosa, G., Focsaneanu, K. S., McLean, J. R. N., McNamee, J. P. & Scaiano, J.C.
798 Photophysical properties of fluorescent DNA-dyes bound to single-and double-stranded DNA
799 in aqueous buffered solution. *Photochem. Photobiol.* **73,** 585-599 (2001).
800 80. Smith, D. C. & Azam, F. A simple, economical method for measuring bacterial protein
801 synthesis rates in seawater using ^{3}H-leucine. *Mar. Microb. Food Webs* **6**, 107-114 (1992).
802 81. Herndl, G. J. et al. Contribution of Archaea to total prokaryotic production in the deep
803 Atlantic Ocean. *Appl. Environ. Microbiol.* **71**, 2303-2309 (2005).
804 82. Garneau, M-E., *et al.* Hydrocarbon biodegradation by Arctic sea-ice and sub-ice
805 microbial communities during microcosm experiments, Northwest Passage (Nunavut,
806 Canada). *FEMS Microbiol Ecol.* **92**, 2016, fiw130 (2016).
807 83. Caporaso, J. G. *et al.* QIIME allows analysis of high-throughput community sequencing
808 data. *Nature Methods* **7**, 335–336 (2010).
809 84. Quince, C. Lanzen, A. Davenport, R. J. & Turnbaugh, P. J. Removing noise from
810 pyrosequenced amplicons. *BMC Bioinformatics* **12**, 38 (2011).

85. Edgar, R. C., Haas, B. J., Clemente, J. C., Quince, C. & Knight, R. UCHIME improves sensitivity and speed of chimera detection. *Bioinformatics* **27**, 2194-2200 (2011).

86. Wang, Q., Garrity, G. M., Tiedje, J. M. & Cole, J. R. Naive Bayesian classifier for rapid assignment of rRNA sequences into the new bacterial taxonomy. *Appl. Environ. Microbiol.* **73**, 5261–5267 (2007).

87. Rognes T., Flouri, T., Nichols, B., Quince, C., Mahé, F. VSEARCH: a versatile open source tool for metagenomics *PeerJ*.: 4: e2584. (2016) doi: 10.7717/peerj.2584

88. Bray, J. C. & Curtis, J. T. An ordination of the upland forest communities of southern Wisconsin. *Ecol. Monogr.*, **27**: 325–349 (1957).